

---

# Terrestrial Planet Formation in Binary Star Systems

Elisa V. Quintana<sup>1</sup> and Jack J. Lissauer<sup>2</sup>

<sup>1</sup> SETI Institute, 515 N. Whisman Road, Mountain View, CA 94043, USA  
[equintana@mail.arc.nasa.gov](mailto:equintana@mail.arc.nasa.gov)

<sup>2</sup> Space Science and Astrobiology Division 245-3, NASA Ames Research Center,  
Moffett Field, CA 94035, USA

## 1 Introduction

More than half of all main sequence stars, and an even larger fraction of pre-main sequence stars, reside in binary/multiple star systems [1, 2]. Numerical simulations of the collapse of molecular cloud cores to form binary stars suggest that disks form within binary star systems [3]. The presence of disk material has been indirectly observed around one or both components of some young binary star systems [2]. Terrestrial planets and the cores of giant planets are thought to form by an accretion process within a disk of dust and gas [4, 5], and therefore may be common in binary star systems. A lower limit of 30 (Jupiter mass) extrasolar planets have been detected in so-called S-type orbits which encircle one member of a binary star system. Most of these extrasolar planets orbit stars whose stellar companion is quite far away, but 3 are in systems with stellar semimajor axes,  $a_B$ , of only  $\sim 20$  AU. The effect of the stellar companion on the formation of these planets remains uncertain. Terrestrial planets have yet to be detected in P-type orbits (which encircle both components) of a main-sequence binary star system, but close binaries are not included in precise Doppler radial velocity search programs because of their complex and varying spectra. The presence of Earth-like exoplanets in main sequence single or binary star systems has yet to be determined, though projects that focus on searching for extrasolar terrestrial planets are currently in development<sup>3</sup> and could begin to provide insight within the next few years.

We have numerically simulated the final stages of terrestrial planet formation in both S-type and P-type orbits within main-sequence binary star systems using two symplectic integration algorithms that we developed for this purpose [6]. Runs are performed using various values for the stellar masses and orbital parameters in order to determine whether/where terrestrial planets can form. Multiple simulations are performed of each binary star system

---

<sup>3</sup> see [www.kepler.arc.nasa.gov](http://www.kepler.arc.nasa.gov)

under study to account for the chaotic nature of these  $N$ -body systems, and we statistically compare the resulting planetary systems formed to those that form in simulations of the Sun-Jupiter-Saturn system which begin with near identical initial disk conditions. We show that (at least the final stages of) terrestrial planet formation can indeed take place in a wide variety of binary star systems, and we have begun to delineate the range of binary star parameter space (masses and orbits) for which Earth-like planets may grow. In this chapter, we present a summary of the results of our simulations of planetary growth in S-type orbits around each star in the  $\alpha$  Centauri system (§2), in other ‘wide’ binary star systems (§3), and in P-type orbits around both stars in close short-period binary star systems (§4). Details of the algorithms that we helped to develop and the corresponding performance tests are presented in Chambers ([6]) and in the previous chapter. Details of our research in terrestrial planet formation in binary star systems are provided in [7, 8, 9, 10, 11, 12]. The results from all of our simulations presented in this chapter (as well as simulations of planetary growth around single stars) can be scaled for different star and disk parameters with the formulae presented in Appendix C of [11].

## 2 Model and Initial Conditions

Our simulations are based on the conventional model of planet formation in which terrestrial planets form via pair-wise accretion of rocky bodies from within a disk of gas and dust that has remained around a newly formed star [4, 5]. For all of our simulations, we assume that rocky Moon-to-Mars-sized planetesimals/embryos have already accreted from within a disk of gas and dust. The initial conditions and physical assumptions of the bodies in the ‘bimodal’ disk are based upon simulations of the final stages of terrestrial planet growth around single stars [13]. Although this formulation is not complete, nor definitive, it provides a model that reproduces our terrestrial planet system (albeit with somewhat larger eccentricities) and can thus be used as a reference point. A comparison between our results and those of the single-star accretion simulations will help to delineate the effects of the binary star system on the accretion process despite our approximations, e.g., the lack of very small bodies and the assumption of perfectly inelastic collisions.

This initial bimodal disk mass distribution adopted from Chambers [13] is used for all of the simulations presented in this chapter. In this disk model, half of the disk mass is composed of 14 rocky embryos (each with a mass of 0.0933 times the mass of the Earth,  $M_{\oplus}$ ), while the remaining mass is distributed equally among 140 planetesimals (each with a mass of 0.00933  $M_{\oplus}$ ). The total disk mass is  $\sim 2.6 M_{\oplus}$ . The profile of the surface density has the form  $a^{-3/2}$  (where  $a$  is the semimajor axis), normalized to 8 g/cm<sup>2</sup> at 1 AU, and follows from models of the minimum mass solar nebula. The bodies are distributed between 0.36 AU and 2.05 AU, and the radius of each body is calculated

assuming a material density of  $3 \text{ g cm}^{-3}$ . The embryos/planetesimals begin with initial eccentricities  $e \leq 0.01$ , inclinations  $i \leq 0.5^\circ$ , and specific initial orbital elements were chosen at random from specified ranges; the same set of randomly selected values was used for all simulations.

The evolution of the accreting bodies subject to gravitational perturbations from both stars and to gravitational interactions and completely inelastic collisions among the bodies is followed for 200 Myr – 1 Gyr. Because these  $N$ -body systems are chaotic in nature, we performed multiple integrations of each system with a slight change in the initial conditions of one body in the disk. This tactic allows us to sample the range of possible outcomes for effectively equivalent initial conditions, and the result is a distribution of final planetary systems.

### 3 Planet Formation in the $\alpha$ Centauri AB Binary Star System

We first examined the late stage of planet formation in the  $\alpha$  Centauri system, which is comprised of a central binary consisting of the G2 star  $\alpha$  Cen A ( $1.1 M_\odot$ ) and the K1 star  $\alpha$  Cen B ( $0.91 M_\odot$ ) [7]. The stars have an orbital semimajor axis of 23.4 AU and an eccentricity of 0.52. The M5 star  $\alpha$  Cen C (Proxima Centauri) is thought to orbit this pair, but at a very large distance (12,000 AU), and is neglected in our simulations. Observations at the Anglo-Australian telescope imply that no planet orbiting either star induces periodic velocity variations as large as 2 m/s (G. Marcy, personal communication, 2006). This upper bound, combined with dynamical stability calculations [15], implies that any planet in an S-type orbit around either component of the  $\alpha$  Cen AB binary must have a mass less than that of Saturn or orbit in a plane that is substantially inclined to the line of sight to the system. Herein we present the results of simulations of the late stages of terrestrial planet growth around  $\alpha$  Cen A and  $\alpha$  Cen B for various initial inclinations of the circumstellar disk relative to the binary orbital plane.

In the majority of our simulations, the circumstellar disk is centered around  $\alpha$  Centauri A with  $\alpha$  Cen B perturbing the system. The initial inclination of the midplane of the disk,  $i$ , begins at either  $0^\circ$ ,  $15^\circ$ ,  $30^\circ$ ,  $45^\circ$ ,  $60^\circ$ , or  $180^\circ$  relative to the plane containing  $\alpha$  Cen A and B. Although a stellar companion present during the earlier stages of planet formation would likely force the planetesimal disk into the plane of the binary orbit, many binary stars may originate as unstable triple star systems which could produce a binary star system with an accretion disk at a high relative inclination. It is also possible that a companion may have been captured around a single star that possesses an accretion disk. The longitude of periastron of the stellar companion is set to either  $90^\circ$  or  $180^\circ$  for each run. We also performed a set of integrations with the disk centered around  $\alpha$  Cen B, with  $\alpha$  Cen A orbiting the system in the same plane and direction ( $i = 0^\circ$ ). For comparison purposes,

we performed a set of runs which follow the evolution of the bimodal accreting disk around the Sun with neither giant planets nor a stellar companion perturbing the system.

Figure 1 shows the results from a simulation in which the disk is centered around  $\alpha$  Cen A and coplanar to the binary orbital plane. Each panel shows the eccentricity of each body in the disk as a function of semimajor axis at the specified time, and the radius of each symbol is proportional to the radius of the body that it represents. Within 100 Myr of the integration, five terrestrial planets that are at least as massive as the planet Mercury have formed around  $\alpha$  Cen A, with a single planetesimal remaining in a highly eccentric orbit. The planetesimal is ejected from the system soon thereafter (110 Myr), and the five terrestrial planets remain on stable orbits within 2 AU for the remainder of the 200 Myr simulation.

The simulation shown in Figure 2 begins with nearly identical initial conditions as the system in Figure 1, with the exception of a small (1 meter) shift in the initial position of one planetesimal near 1 AU. Although the early evolution of the disk is qualitatively similar among the two systems, they diverge with a Lyapunov time of order  $10^2$  years ([12]). In the simulation shown in Figure 2, this divergence ultimately leads to the formation of an substantially different planetary system: four terrestrial planets form within 1.8 AU of  $\alpha$  Cen A. Although these  $N$ -body simulations are highly stochastic, there are clear trends in the final planetary systems (number, masses, orbits etc.) that form in simulations with the same binary star parameters (as will be shown further in §4 and 5).

Figure 3 shows the results of an integration in which the disk is initially inclined by  $15^\circ$  relative to the binary orbital plane. With a higher initial disk inclination (than the simulations shown in the previous two figures), the bodies in the disk are more dynamically excited, and more mass is lost from the system. In this case, nearly 15% more mass is lost than the  $i = 0^\circ$  simulations, and three terrestrial planets (as well as a single planetesimal) remain by the end of the integration.

We performed a total of 16 simulations of terrestrial planet growth around  $\alpha$  Cen A in which the midplane of the disk was initially inclined by  $30^\circ$  or less relative to the binary orbital plane. In these simulations, when the bodies in the disk began in prograde orbits, from 3 – 5 terrestrial planets formed around  $\alpha$  Cen A. Slightly more formed, from 4 – 5, when  $i = 180^\circ$  relative to the binary plane. From 2 – 4 planets formed in a disk centered around  $\alpha$  Cen B, with  $\alpha$  Cen A perturbing the system in the same plane. The final planetary systems that form in all of these simulations are shown in Figures 8 – 10 in [7]. The distribution of final terrestrial planet systems in the aforementioned cases is quite similar to that produced by calculations of terrestrial planet growth in the Sun-Jupiter-Saturn system.

In contrast, terrestrial planet growth around a star lacking both stellar and giant planet companions is slower and extends to larger semimajor axis for the same initial disk of planetary embryos (see Figure 12 in [7]). In systems

with the accreting disk initially inclined at  $45^\circ$  to the binary plane, from 2 – 5 planets formed, despite the fact that more than half of the disk mass was scattered into the central star. When the disk was inclined by  $60^\circ$ , the stability of the planetary embryos decreased dramatically, and almost all of the planetary embryos and planetesimals were lost from these systems (e.g., Figure 6 in [7]). Figures of the temporal evolution of each of our  $\alpha$  Cen simulations can be found in [7, 9].

#### 4 S-type Orbits in Other ‘Wide’ Binary Star Systems

In this section we present the results from a survey ( $\sim 120$  numerical simulations) on the effects of a stellar companion on the final stages of terrestrial planet formation in S-type orbits around one component of a binary star system [12]. We examine binary star systems with stellar mass ratios  $\mu \equiv M_C/(M_\star + M_C) = 1/3, 1/2, \text{ or } 2/3$ , where  $M_\star$  is the mass of the star around which the protoplanetary disk is situated, and  $M_C$  is the mass of the companion. The majority of our simulations begin with equal mass stars ( $\mu = 1/2$ ) of either  $M_\star = M_C = 0.5 M_\odot$  (Set A) or  $M_\star = M_C = 1 M_\odot$  (Set B). Simulations were also performed with a more massive ‘primary’ star (the one the disk is centered around),  $M_\star = 1 M_\odot$  and  $M_C = 0.5 M_\odot$  ( $\mu = 1/3$ , Set C), and also with a smaller ‘primary’ star of  $M_\star = 0.5 M_\odot$  and a more massive companion  $M_C = 1 M_\odot$  ( $\mu = 2/3$ , Set D). The stellar semimajor axis,  $a_B$ , and binary eccentricity,  $e_B$ , are chosen such that the binary periastron takes one of the three values,  $q_B = 5 \text{ AU}, 7.5 \text{ AU}, \text{ or } 10 \text{ AU}$ . Note that binary systems with much wider periastra would have little effect on terrestrial planet formation, whereas systems with significantly smaller periastra would completely destroy the initial disk of planetesimals. The binary stars are separated by  $a_B = 10 \text{ AU}, 13\frac{1}{3} \text{ AU}, 20 \text{ AU}, \text{ or } 40 \text{ AU}$ , and the eccentricities are varied in the range  $0 \leq e_B \leq 0.875$ . The largest semimajor axis for which particles can be stable in any of the systems that we explore is 2.6 AU; we therefore omit giant planets (those in the Solar System in orbit beyond 5 AU) from our integrations.

For our accretion simulations, our exploration of parameter space has two coupled goals. On one hand, we want to determine the effects of the binary orbital elements on the final terrestrial planet systems produced. On the other hand, for a given binary configuration, we want to explore the distribution of possible resulting planetary systems (where the results must be described in terms of a distribution due to the sensitive dependence on the initial conditions). We have performed from 3 – 30 integrations for each wide binary star configuration ( $\mu, a_B$ , and  $e_B$ ) considered herein, with small differences in the initial conditions: a single planetesimal is moved forward along its orbit by a small amount (1 – 9 meters) in an orbit near either 0.5, 1, or 1.5 AU, prior to the integration. Ideally, of course, one would perform larger numbers of integrations to more fully sample the distributions of results, but computer resources limit our sample size. Figures (similar to Figures 1 – 3) of the evo-

lution of most wide binary star systems that we simulated can be found in [10, 9, 12].

The stellar mass ratio,  $\mu$ , and the periastron distance  $q_B$  strongly influence where terrestrial planets can form in ‘wide’ binary star systems. The effect of  $q_B$  on the distribution of final planetary system parameters (i.e., number, masses, etc.) is demonstrated in Figures 4 – 6. The semimajor axis of the outermost planet can be used as a measure of the size of the terrestrial planet system. Figure 4 shows the distribution of the semimajor axis of the outermost final planet formed in each simulation for systems with  $q_B = 5$  AU (top panel), 7.5 AU, (middle panel), and 10 AU (lower panel). Note that twice as many integrations have been performed in Set B (shown in light gray) as in Set A (dashed bars). Figure 4 shows a clear trend: as the binary periastron increases, the distribution of semimajor axes (of the outermost planet) becomes wider and its expectation value shifts to larger values. The distributions of the total number of final planets formed are shown in Figure 5 for simulations with  $q_B = 5$  AU, 7.5 AU, and 10 AU. In general, a smaller binary periastron results in a larger percentage of mass loss, and a smaller number of final planets. From 1 – 3 planets formed in all systems with  $q_B = 5$  AU, 1 – 5 planets remained in systems with  $q_B = 7.5$  AU, and 1 – 6 planets formed in all systems with  $q_B = 10$  AU. The range in the number of possible planets grows with increasing binary periastron; similarly, the average number of planets formed in the simulations is an increasing function of  $q_B$ . In the  $q_B = 7.5$  AU set with equal mass stars of  $1 M_\odot$ , an average of 2.8 planets formed in the distribution of our largest set of 30 integrations. The distribution extends farther out if the perturbing star is smaller relative to the central star for a given stellar mass ratio, and slightly farther out when the stars are more massive relative to the disk. Figure 6 shows the distribution of final planetary masses (in units of the Earth’s mass,  $M_\oplus$ ) formed in systems with  $q_B = 5$  AU, 7.5 AU, and 10 AU. The median mass of the final planets doesn’t depend greatly on  $q_B$ . This result suggests that planet formation remains quite efficient in the stable regions, but that the size of the stable region shrinks as  $q_B$  gets smaller. This trend is consistent with the decline in the number of planets seen in Figure 5. When the periastron value becomes as small as 5 AU, planets only form within 1 AU, and the mass distribution tilts toward  $m_p < M_\oplus$ , i.e., the formation of Earth-like planets is compromised.

## 5 P-type Orbits Within Close Binary Star Systems

Herein we present results from simulations of the late stages of terrestrial planet formation within a circumbinary disk surrounding various short-period binary systems. For a more extensive discussion, see Quintana & Lissauer ([11]). The combined mass of the binary stars is equal to  $1 M_\odot$  in all of these simulations, with the stellar mass ratio  $\mu$  equal to either 0.2 or 0.5. Binary star separations in the range  $a_B = 0.05$  AU – 0.4 AU are examined, while  $e_B$

begins at 0, 1/3, 0.5, or 0.8 such that the stellar apastron  $Q_B \equiv a_B(1 + e_B)$  is  $0.05 \text{ AU} \leq Q_B \leq 0.4 \text{ AU}$ . For most of the simulations, the midplane of the circumbinary disk begins coplanar to the stellar orbit, but for one set of binary star parameters a relative inclination of  $i = 30^\circ$  is investigated. The initial disk of planetary embryos/planetesimals is the same as that used for simulating accretion within our Solar System [13], in the  $\alpha$  Centauri AB system (§3), and in wide binary star systems (§4). Giant planets with masses and initial orbits equal to those of Jupiter and Saturn at the present epoch are included in the simulations, as they are in most simulations of the late stages of terrestrial planet accumulation in our Solar System. We use a ‘close-binary’ algorithm which follows the accretion evolution of each body in the disk relative to the center of mass of the binary star system. To account for the stochastic nature of these simulations, each binary star system under study is simulated five or six times with slightly different initial conditions for the circumbinary disk. We statistically compared our results to a large set ( $> 30$ ) of simulations of the Sun-Jupiter-Saturn system that began with virtually the same initial disk mass distribution [13, 11].

Figure 7 shows the evolution of the circumbinary disk centered around two  $0.5 M_\odot$  binary stars with  $a_B = 0.1 \text{ AU}$  and in a circular orbit. The initial disk is the same as that shown in the first panel of Figure 1, planetary embryos and planetesimals are represented by circles whose sizes are proportional to the physical sizes of the bodies, and the locations of the circles show the orbital semimajor axes and eccentricities of the represented bodies relative to center of mass of the binary stars. The perturbations on the inner edge of the disk are apparent within the first million years, and in this case five terrestrial planets have formed within 100 Myr, and continue on stable orbits for the remainder of the 500 Myr integration. Figures 8 and 9 show the results from two simulations with equal ( $0.5 M_\odot$ ) mass stars. In Figure 8 the stellar separation is  $a_B = 0.2 \text{ AU}$  and  $e_B = 0.5$  ( $Q_B = 0.3$ ), while in Figure 9 the stars are separated by  $a_B = 0.3 \text{ AU}$  and have an eccentricity of  $e_B = 1/3$  ( $Q_B = 0.4$ ). In both simulations, more than 70% of the initial disk mass was lost from the system within the first 50 Myr, and each simulation resulted in a single planet that is at least as massive as the planet Mercury. The evolution of most of the close binary star simulations are presented in [10, 9, 11], and [11] provides a statistical comparison of the planets that form around each binary star configuration to those that form around the Sun (with giant planets included in each case).

Figure 10 show the distributions in the semimajor axis of the innermost planets that formed for systems that began on initially circular orbits (gray bars) and for those in which the binary star eccentricity ranged from  $1/3 \geq e_B \geq 0.8$ . For the zero-eccentricity simulations, there is a clear separation at  $\sim 1 \text{ AU}$  among systems with  $Q_B \leq 0.2 \text{ AU}$  and  $Q_B \geq 0.3 \text{ AU}$ . The distributions of the innermost semimajor axes of the planets formed in binary stars that began with higher eccentricities are wider, as each set of these simulations resulted in at least one system with 1 – 2 final planets, as shown in Figure

11. Figure 12 shows the distributions of the final masses of the planets formed among binary star systems with different apastron values. Earth-mass planets only formed in our simulations in which  $Q_B \leq 0.2$  AU.

In summary, close binary stars with maximum separations  $Q_B \leq 0.2$  AU and small  $e_B$  had little effect on the accreting bodies, and in most of these simulations terrestrial planets formed over essentially the entire range of the initial disk mass distribution (and even beyond 2 AU in many cases). The stellar perturbations cause orbits to precess, thereby moving secular resonances out of the inner asteroid belt, allowing terrestrial planets to form from our initially compact disk and remain in stable orbits as far as 2.98 AU from the center of mass of the binary stars. The effects of the stellar perturbations on the inner edge of the planetesimal disk became evident in systems with larger  $a_B$  (and  $Q_B \gtrsim 0.3$  AU) and in most of the simulations with  $e_B > 0$ . Terrestrial-mass planets can still form around binary stars with nonzero eccentricity, but the planetary systems tend to be sparser and more diverse. Binary stars with  $Q_B \gtrsim 0.3$  AU perturb the accreting disk such that the formation of Earth-like planets near 1 AU is unlikely. Despite these constraints, at least one terrestrial planet (at least as massive as the planet Mercury) formed in each of our simulations.

## 6 Conclusions

Our exploration of parameter space shows how binary orbital parameters affect terrestrial planet formation. We find that the presence of a binary companion of order 10 AU away acts to limit the number of terrestrial planets and the spatial extent of the terrestrial planet region around one member of a binary star system, as shown by Figures 3 – 5. To leading order, the periastron value  $q_B$  is the most important parameter in determining binary effects on planetary outcomes in wide-binary star systems (more predictive than  $a_B$  or  $e_B$  alone), whereas  $Q_B$  is the most influential parameter for accretion within circumbinary disks. In our ensemble of  $> 100$  wide binary star simulations that began with equal mass stars, from 1 – 6 planets formed with semimajor axes  $\lesssim 2.2$  AU of the central star in binary systems with  $q_B = 10$  AU, from 1 – 5 planets formed within 1.7 AU for systems with  $q_B = 7.5$  AU, and from 1 – 3 planets formed within 0.9 AU when  $q_B = 5$  AU. For a given binary periastron  $q_B$ , fewer planets tend to form in binary systems with larger values of  $(a_B, e_B)$ , as shown in Figure 5.

Binary companions also limit the extent of the terrestrial planet region in nascent planetary systems orbiting one member of the stellar pair. As shown in Figures 4 – 6, wider binaries allow for larger systems of terrestrial planets. Although the binary periastron is the most important variable in determining the extent of the final system of terrestrial planets (as measured by the semimajor axis of the outermost planet), for a given periastron, the sizes of the terrestrial planet systems show a wide distribution. In these simulations,

the initial disk of planetesimals extends out to 2 AU, so we do not expect terrestrial planets to form much beyond this radius. For binary periastron  $q_B = 10$  AU, the semimajor axis of the outermost planet typically lies near 2 AU, i.e., the system explores the entire available parameter space for planet formation. Since these results were obtained with equal mass stars (including those with  $M = 1.0 M_\odot$ ), we conclude that the constraint  $q_B \gtrsim 10$  AU is sufficient for binaries to leave terrestrial planet systems unperturbed. With smaller binary periastron values, the resulting extent of the terrestrial planet region is diminished. When binary periastron decreases to 5 AU, the typical system extends only out to  $a_p \sim 0.75$  AU and no system has a planet with semimajor axis beyond 0.9 AU (but note that we did not perform simulations with  $q_B = 5$  AU and small  $e_B$ ).

While the number of forming planets and their range of orbits is restricted by binary companions, the masses and eccentricities of those planets are much less affected. The distribution of planet masses is nearly independent of binary periastron (see Figure 6), although the wider binaries allow for a few slightly more massive terrestrial planets to form. Finally, we note that the time scales required for terrestrial planet formation in these systems lie in the range 50 – 200 Myr, consistent with previous findings [13, 7, 11], and largely independent of the binary properties. This result is not unexpected, as the clock for the accumulation of planetesimals is set by their orbit time and masses [4], and not by the binary orbital period.

This work has important implications regarding the question of what fraction of stars might harbor terrestrial planetary systems. The majority of solar-type stars live in binary systems, and as shown in this chapter, binary companions can disrupt both the formation of terrestrial planets and their long term prospects for stability. Approximately half of the known binary systems are wide enough (in this context, having sufficiently large values of periastron) so that Earth-like planets can remain stable over the entire 4.6 Gyr age of our Solar System [16, 17]. For the system to be stable out to the distance of Mars’s orbit, the binary periastron  $q_B$  must be greater than about 7 AU, and about half of the observed binaries have  $q_B > 7$  AU. Our work on the formation of terrestrial planets shows similar trends. When the periastron of the binary is larger than about  $q_B = 10$  AU, even for the case of equal mass stars, terrestrial planets can form over essentially the entire range of orbits allowed for single stars (out to the edge of the initial planetesimal disk at 2 AU). When periastron  $q_B < 10$  AU, however, the distributions of planetary orbital parameters are strongly affected by the presence of the binary companion (see Figures 7 – 12). Specifically, the number of terrestrial planets and the spatial extent of the terrestrial planet region both decrease with decreasing binary periastron. When the periastron value becomes as small as 5 AU, planets no longer form with  $a = 1$  AU orbits and the mass distribution tilts toward  $m_p < 1M_\oplus$ , i.e., the formation of Earth-like planets is compromised.

Given the enormous range of orbital parameter space sampled by known binary systems, from contact binaries to separations of nearly a parsec, the

range of periastron where terrestrial planet formation is affected is quite similar to the range of periastron where the stability of Earth-like planets is compromised. As a result,  $\sim 40 - 50\%$  of binaries are wide enough to allow both the formation and the long term stability of Earth-like planets in S-type orbits encircling one of the stars. Furthermore, approximately 10% of main sequence binaries are close enough to allow the formation and long-term stability of terrestrial planets in P-type circumbinary orbits ([16, 11]). Given that the galaxy contains more than 100 billion star systems, and that roughly half remain viable for the formation and maintenance of Earth-like planets, a large number of systems remain habitable based on the dynamic considerations of this research.

## 7 Acknowledgements

We thank Michael J. Way for providing additional CPUs at NASA ARC. E.V.Q. received support in various stages of this research from NASA GSRP, NAS/NRC and NASA NPP fellowships, and the University of Michigan through the Michigan Center for Theoretical Physics (MCTP). J.J.L. is supported in part by the NASA Astrobiology Institute under the NASA Ames Investigation “Linking our Origins to our Future”.

## References

1. Duquennoy, A., & Mayor, M. 1991, *A&A*, 248, 485
2. Mathieu, R. D., Ghez, A. M., Jensen, E. L. N., & Simon M. 2000, in *Protostars and Planets IV*, ed. V. Mannings, A. P. Boss, & S. S. Russell (Tucson: Univ. of Arizona Press), 703
3. Bodenheimer, P., Hubickyj, O., & Lissauer, J. J. 2000, *Icarus*, 143, 2
4. Safronov, V. S., 1969. *Evolution of the Protoplanetary Cloud and Formation of the Earth and the Planets* (Moscow: Nauka Press).
5. Lissauer, J. J. 1993, *Ann. Rev. Astron. Astrophys.*, 31, 129
6. Chambers, J. E., Quintana, E. V., Duncan, M. J., & Lissauer, J. J. 2002, *AJ*, 123, 2884
7. Quintana, E. V., Lissauer, J. J., Chambers, J. E., & Duncan, M. J. 2002, *ApJ*, 576, 982
8. Quintana, E. V. 2003, in *ASP Conf. Ser. 294, Scientific Frontiers in Research on Extrasolar Planets*, ed. Deming, D., & Seager, S. (San Francisco: ASP), 319
9. Quintana, E. V. 2004, *Planet Formation in Binary Star Systems*, Thesis (Ph.D.), University of Michigan, Ann Arbor (Ann Arbor: UMI Company)
10. Lissauer, J. J., Quintana, E. V., Chambers, J. E., Duncan, M. J., & Adams, F. C. 2004, *RevMexAA*, 22, 99
11. Quintana, E. V., & Lissauer, J. J. 2006, *Icarus*, 185, 1
12. Quintana, E. V., F. C. Adams, J. J. Lissauer, & J. E. Chambers 2007, *Ap.J.*, 660, 807
13. Chambers, J. E. 2001, *Icarus*, 152, 205

14. Endl, M., Kurster, M., Els, S., Hatzes, A. P., & Cochran, W. D. 2001, *A&A*, 374, 675
15. Wiegert, P. A., & Holman, M. J. 1997, *AJ*, 113, 1445
16. David, E., Quintana, E. V., Fatuzzo, M., & Adams, F. C. 2003, *PASP*, 115, 825
17. Fatuzzo, M., Adams, F. C., Gauvin, R., & Proszkow, E. M. 2006, *PASP*, 118, 1510

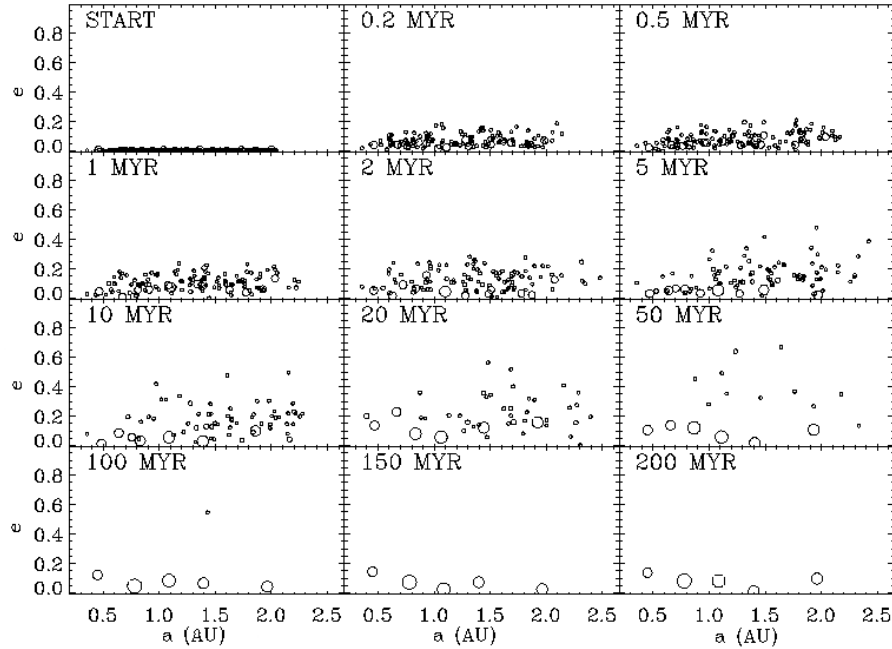


**Fig. 1.** The temporal evolution of planetary embryos/planetesimals in a circumstellar disk centered around  $\alpha$  Cen A and coplanar with the binary orbital plane (simulation AC*i*0\_3 in [7]). The radius of each symbol is proportional to the radius of the body that it represents, and the eccentricities are displayed as a function of semimajor axis. By the end of the 200 Myr integration, five terrestrial planets have formed within 2 AU of  $\alpha$  Cen A, accumulating  $\sim 89\%$  of the initial disk mass. Figures 1 and 2 from [7] show the results of two simulations that begin with the same stellar parameters (runs AC*i*0\_1 and AC*i*0\_2), but with slightly different initial disk conditions.

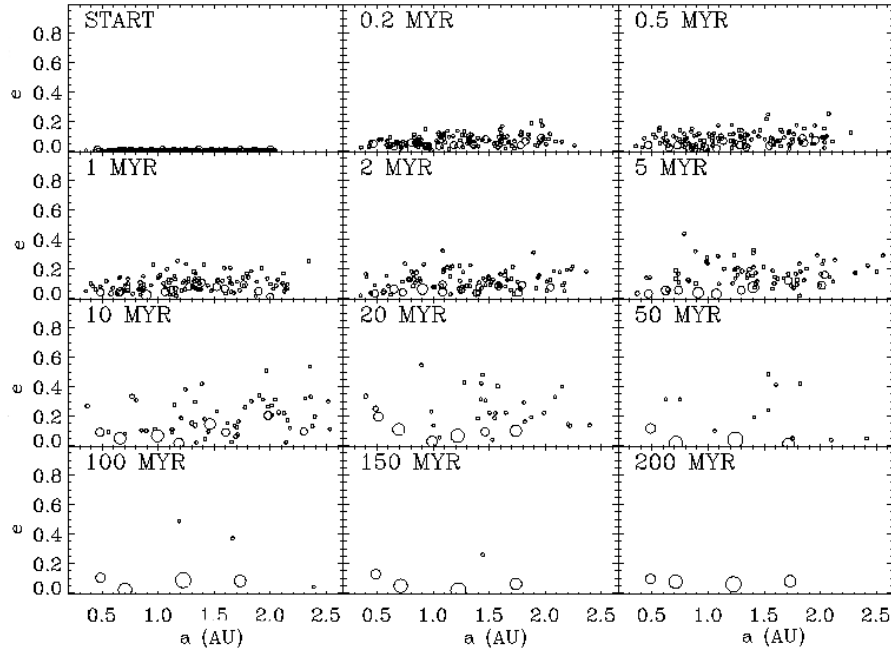


**Fig. 2.** The temporal evolution of virtually the same circumstellar disk around  $\alpha$  Cen A as that shown in Figure 1, but in this case a single planetesimal near 1 AU is shifted by a small amount (1 meter along its orbit) prior to the integration (simulation AC*i*0\_4 in [7]). The stellar parameters and all other disk initial conditions are identical to the system in Figure 1. The dynamics of the disk are generally the same in the earlier stages of the simulations shown here and in Figure 1, as the more massive embryos orbit with low eccentricities whereas the planetesimals are dynamically excited to much higher values. The stochastic nature of these  $N$ -body systems is evident, however, in the final planetary system that formed, and demonstrates the sensitive dependence of the outcome on the initial conditions. Four terrestrial planets, comprised of  $\sim 88\%$  of the initial disk mass, remain within 1.7 AU of  $\alpha$  Cen A. Figures 1 and 2 from [7] show the results of two simulations that begin with the same stellar parameters (runs AC*i*0\_1 and AC*i*0\_2), but with slightly different initial disk conditions.

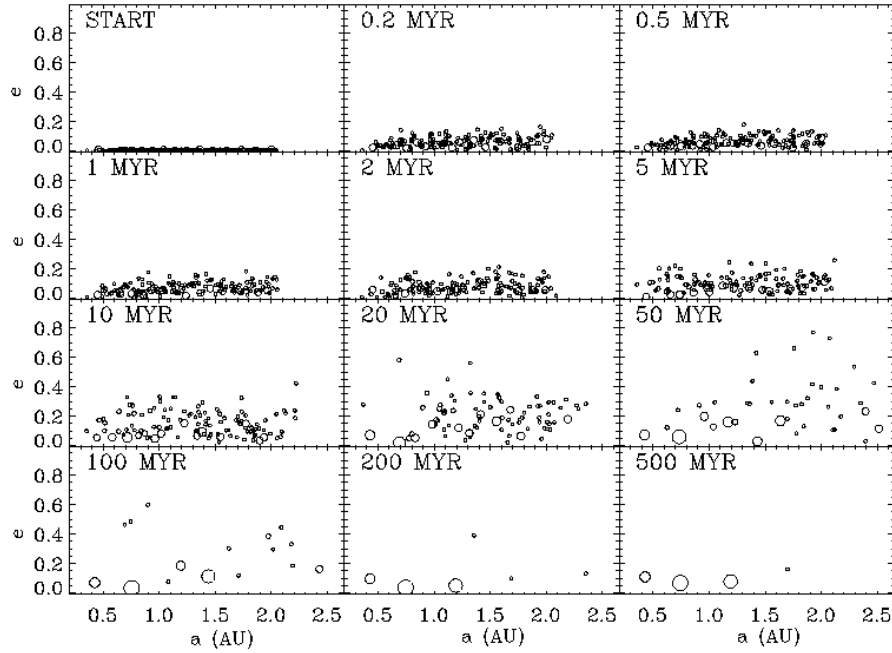


**Fig. 3.** The temporal evolution of our standard circumstellar disk centered around  $\alpha$  Cen A and initially inclined by  $15^\circ$  to the binary orbital plane (simulation AC*i*15\_2 in [7]). The eccentricities of the embryos/planetesimals are displayed as a function of semimajor axis, and the radius of each symbol is proportional to the radius of each body that it represents. In this case, three terrestrial planets formed within  $\sim 1.2$  AU, and a single planetesimal remained exterior to these planets at  $\sim 1.7$  AU, all composed of  $\sim 74\%$  of the initial disk mass. Similar evolution plots for all of the simulations involving  $\alpha$  Cen A and B can be found in [7, 8, 9, 10]

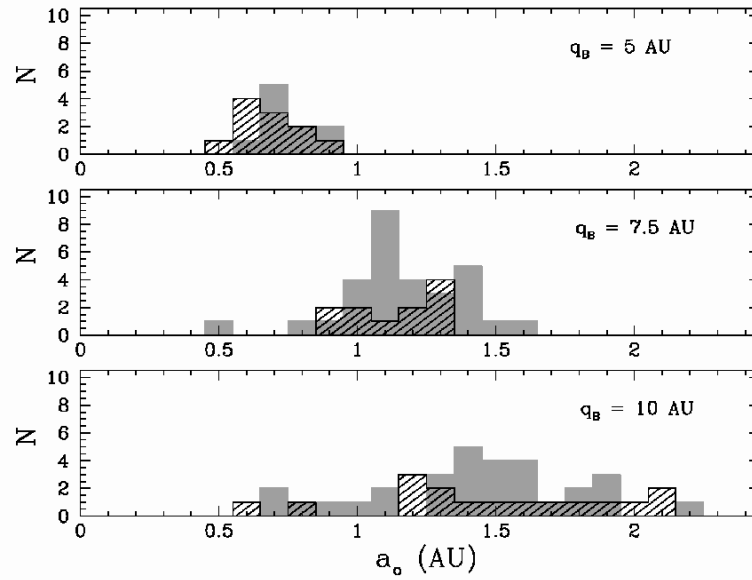


**Fig. 4.** The distribution of the semimajor axis of the outermost final planet,  $a_0$ , formed For binary star systems with  $q_B = 5$  AU (top panel),  $q_B = 7.5$  AU (middle panel), and  $q_B = 10$  AU (bottom panel). The light gray bars represent simulations from Set A with  $M_* = M_C = 0.5 M_\odot$ , whereas the dashed bars represent systems from Set B with  $M_* = M_C = 1.0 M_\odot$ . Although the semimajor axes extend to larger values in binary systems with larger periastron, the inner edge of the distribution is roughly determined by the inner edge of the initial disk of embryos, as in the single star case, i.e., the presence of different stellar companions has a minimal effect on the inner terrestrial region. Note that figures of these distributions (and also those shown in Figures 6 and 7) that include the results from simulations that began with unequal stars ( $\mu \neq 0.5$ ) are presented in [12].

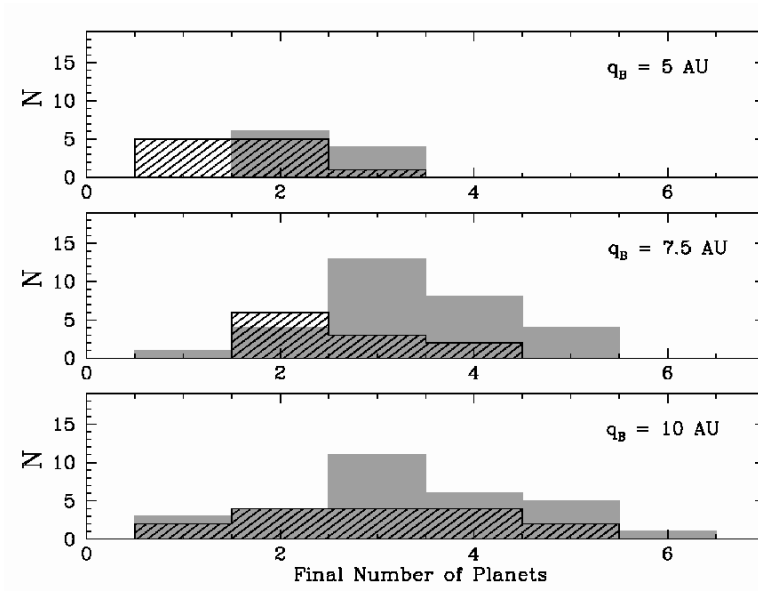


**Fig. 5.** Distributions of the number of final planets formed for binary star systems with  $q_B = 5$  AU (top panel),  $q_B = 7.5$  AU (middle panel), and  $q_B = 10$  AU (bottom panel). The bar types correspond to the different sets of runs as described in Figure 4. The typical number of final planets clearly increases in systems with larger stellar periastron, and also when the companion star is less massive than the primary (for a given stellar mass ratio).

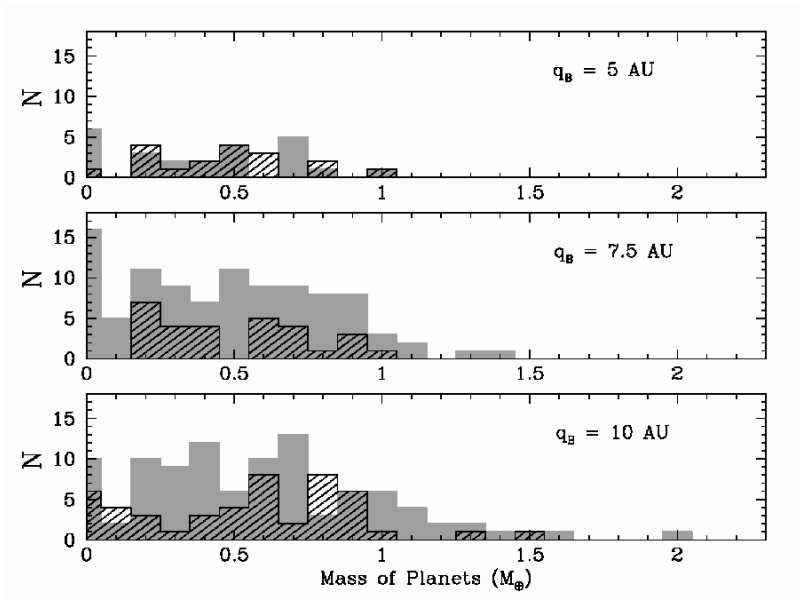


**Fig. 6.** Distributions of the final masses of planets formed within binary star systems with  $q_B = 5 \text{ AU}$  (top panel),  $q_B = 7.5 \text{ AU}$  (middle panel), and  $q_B = 10 \text{ AU}$  (bottom panel). The bar types correspond to the different sets of runs as described in Figure 4. Although the size of the stable region shrinks as  $q_B$  gets smaller, the median mass of the final planets does not vary greatly for a given  $q_B$ , suggesting that planet formation remains efficient in the stable regions.

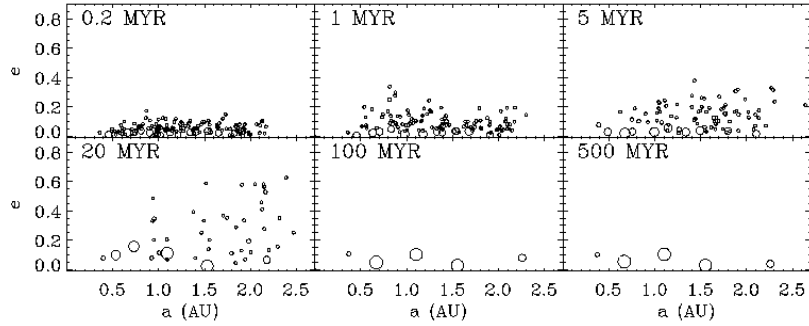


**Fig. 7.** The temporal evolution of the circumbinary disk around binary stars with  $a_B = 0.1$  AU,  $e_B = 0$ , and equal mass stars of  $M_* = 0.5 M_\odot$ . Jupiter- and Saturn-like planets are also included. The planetary embryos and planetesimals are represented by circles whose sizes are proportional to the physical sizes of the bodies. The locations of the circles show the orbital semimajor axes and eccentricities of the represented bodies relative to center of mass of the binary stars. The initially dynamically cold disk heats up during the first 10 Myr, especially in the outer region, where the perturbations of the single giant planet included in this simulation are the greatest. By 100 Myr into the simulation, five planets on low eccentricity orbits have formed and survive for the remainder of the simulation.

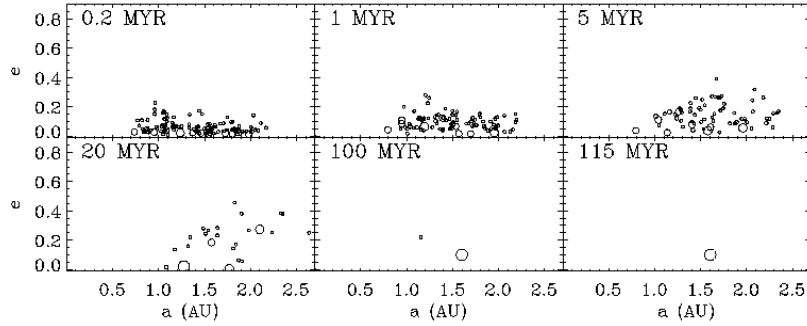


**Fig. 8.** The temporal evolution of simulation that begins with a larger stellar separation ( $a_B = 0.2$  AU) and a higher binary eccentricity ( $e_B = 0.5$  AU) as the system shown in Figures 6. The binary system is composed of equal mass stars of  $M_* = 0.5 M_\odot$ , and Jupiter and Saturn are included. The planetary embryos and planetesimals are represented by circles whose sizes are proportional to the physical sizes of the bodies as in Figure 6. The locations of the circles show the orbital semimajor axes and eccentricities of the represented bodies relative to center of mass of the binary stars. The last ejection occurs at 115 Myr, in which only one planet remains in the system at  $\sim 1.6$  AU.

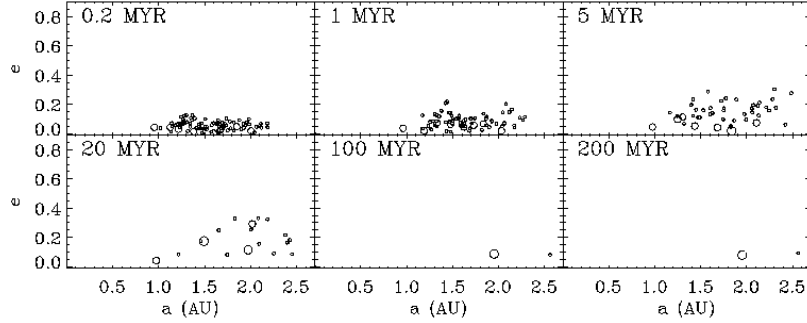


**Fig. 9.** This figure shows the early evolution of the circumbinary disk around binary stars with  $a_B = 0.3$  AU,  $e_B = 1/3$ . The effect of the stellar companion is apparent in the first panel where the inner part of the disk is already substantially excited by 200,000 yr. Eccentricities remain high throughout the evolution, and by 100 Myr only one planet more massive than the planet Mercury has formed in the terrestrial planet zone, and a single planetesimal remains beyond 2.5 AU.

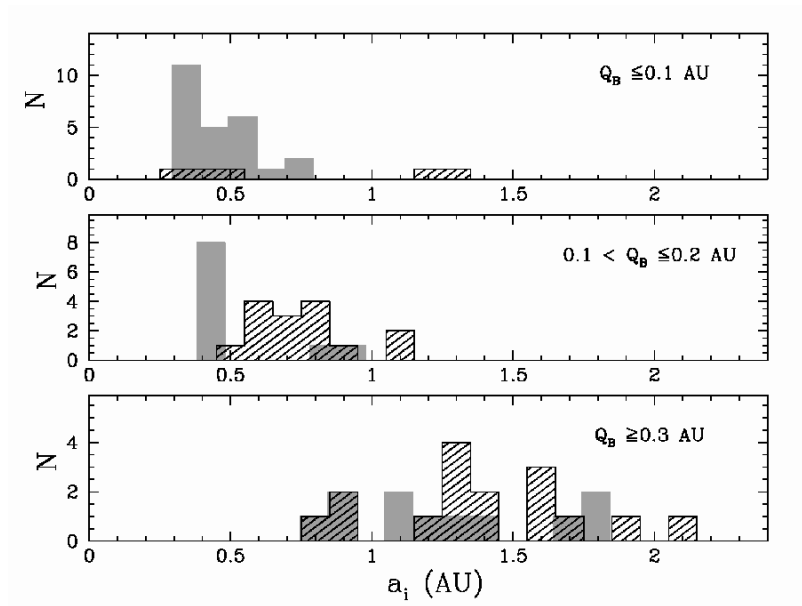


**Fig. 10.** Distributions of the semimajor axis of the innermost final planet,  $a_i$ , formed in binary star systems with  $Q_B \leq 0.1$  AU (top panel),  $0.1 < Q_B \leq 0.2$  AU (middle panel), and  $Q_B \geq 0.3$  AU (bottom panel). The light gray bars represent simulations in which the binary stars began on circular ( $i = 0^\circ$ ) orbits, and the dashed bars represent systems with  $1/3 \geq e_B \geq 0.8$ .

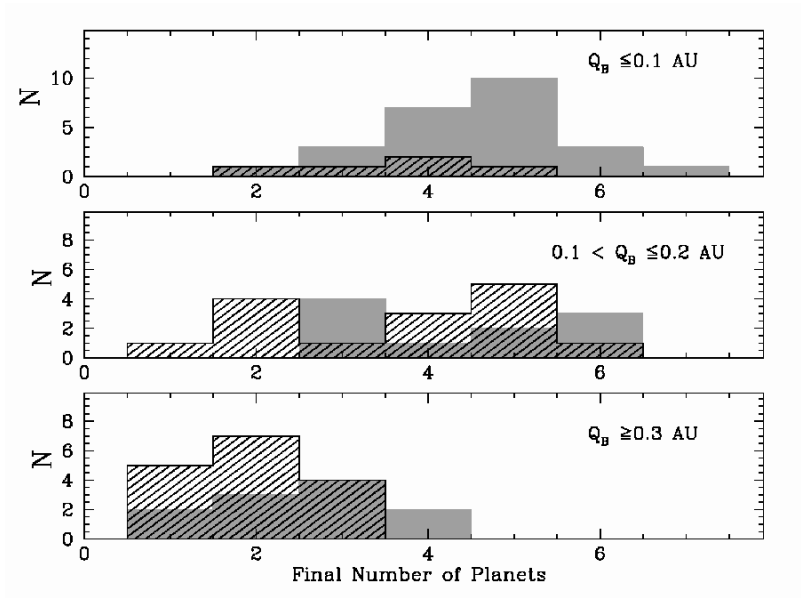


**Fig. 11.** Distributions of the semimajor axis of the innermost final planet,  $a_i$ , formed in binary star systems with  $Q_B \leq 0.1$  AU (top panel),  $0.1 < Q_B \leq 0.2$  AU (middle panel), and  $Q_B \geq 0.3$  AU (bottom panel). The bar types correspond to the different sets of runs as described in Figure 10.

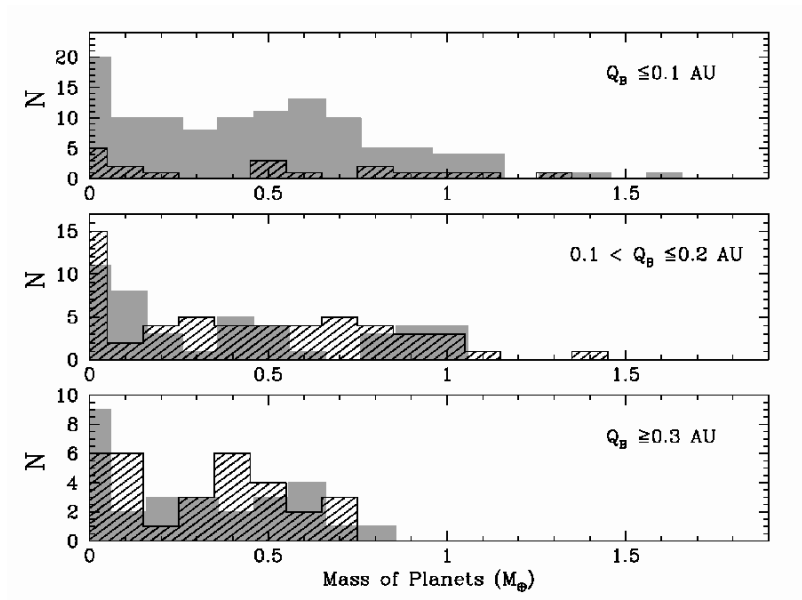


**Fig. 12.** Distributions of the semimajor axis of the innermost final planet,  $a_i$ , formed in binary star systems with  $Q_B \leq 0.1$  AU (top panel),  $0.1 < Q_B \leq 0.2$  AU (middle panel), and  $Q_B \geq 0.3$  AU (bottom panel). The bar types correspond to the different sets of runs as described in Figure 10.